

AD 657371

DOME EFFECTIVENESS AND THE SCALING
AND AREA DEPENDENCE OF
BOUNDARY-LAYER PRESSURE SPECTRA
VIEWED WITH REGARD TO
CHARACTERISTIC WAVENUMBER RANGES

REPORT NO. TRG-011-TN-65-8
DECEMBER 1965

SUBMITTED TO:

CODE 466
OFFICE OF NAVAL RESEARCH
WASHINGTON, D. C. 20360

CONTRACT NO.:

Nonr 4385 (00)

DDC
RECEIVED
SEP 1 1967
RECEIVED
C

This document has been approved
for public release and sale; its
distribution is unlimited.

Reproduced by the
CLEARINGHOUSE
for Federal Scientific & Technical
Information Springfield Va. 22151

TRG CONTROL DATA
DIVISION CORPORATION

535 BROAD HOLLOW ROAD, MELVILLE, NEW YORK 11746 AREA CODE 516/531-0600 TWX 510 224-6438

DOM E EFFECTIVENESS AND THE SCALING AND AREA
DEPENDENCE OF BOUNDARY-LAYER PRESSURE SPECTRA
VIEWED WITH REGARD TO CHARACTERISTIC WAVENUMBER
RANGES

Report No. TRG-011-TN-65-8
Contract No. Nonr 4385(00)

December, 1965

Submitted to:

Code 466
Office of Naval Research
Washington 25, D.C.

Author:


David M. Chase

Approved:


Walton Graham
Head, Systems Department

TRG/A Division of Control Data Corporation
535 Broadhollow Road
Melville, L.I., New York

FOREWORD

The present report constitutes an unclassified version of a classified paper presented at the 23rd Navy Symposium on Underwater Acoustics, Washington, D.C., 30 November - 2 December 1965 (ONR Symp. Rept. ACR-115 (confidential), p.51).

ABSTRACT

Regarding the spectrum of turbulent boundary-layer (TBL) pressure averaged over a flush or shielded area, two distinct wavenumber domains are distinguished: (1) the domain of convective wave numbers $K > \omega/U_\infty$ [U_∞ = asymptotic flow velocity, $\bar{K} = (K_1, K_3)$] such that boundary-layer eddies of frozen shape convected downstream at speed $u \leq U_\infty$ can generate pressure fluctuations of the given frequency; in this domain the wavenumber-frequency spectrum of TBL pressure $P(\bar{K}, \omega)$ has a broad peak; (2) the domain of relatively low wavenumbers where the response function for pressure on the area in question has its largest magnitude. For a circular flush area of radius R_0 , the contribution to the average-pressure spectrum $Q_0(\omega)$ from the high-wavenumber domain, for $\omega R_0/U_\infty \gg 1$, varies as R_0^{-3} . If $P(\bar{K}, \omega)$ averaged over the angle of \bar{K} is substantially constant (wavenumber-white) for most $K \leq 2\pi R_0^{-1}$, the contribution to $Q_0(\omega)$ from the low-wavenumber domain varies rather as R_0^{-2} . A further low-wavenumber contribution due to compressibility ($K \leq \omega/c$, c = sound speed), for $\omega R_0/c \leq 1$, will be independent of R_0 . In the average-pressure spectrum on an area separated from the flow by a fluid layer of depth L , the high-wavenumber contribution is indicated to be reduced relative to an equal flush area much as though averaged not over the actual area πR_0^2 but over the entire lateral area of the layer face; in the limit of a laterally infinite layer, a residual reduction factor $\sim \exp(-2\omega L/U_\infty)$ instead applies. The low-wavenumber contribution is reduced rather as though averaged over an area πR_e^2 (if $R_e \geq R_0$) where $R_e^{-2} = (1/4)[(\omega/c)^2 + (1/4)L^{-2}]$. With reference to noise reduction for an array of shielded elements, the effect of the increased correlation distance is also considered.

Regarding the scaling of TBL pressure on a flush area in the high-frequency range $\omega v/v_*^2 \geq 0.1$, the probable length scale for

the high-wavenumber part is the viscous-sublayer parameter ν/v_* . If this contribution predominates in the point-pressure spectrum $P(\omega)$, the scaling law is $P(\omega) = \rho^2 \nu v_*^2 H_+(\omega \nu / v_*^2)$ with H_+ some function of the dimensionless argument. In the average-pressure spectrum $Q_o(\omega)$ on a large area ($\omega R_o / U_\infty \gg 1$) in the high-frequency range, the high-wavenumber contribution similarly conforms to the scaling law $Q_{o+}(\omega) = (\omega R_o / v_*)^{-3} \rho^2 \nu v_*^2 L_+(\omega \nu / v_*^2)$. The low-wavenumber contribution, if $P(\bar{K}, \omega)$ is wavenumber-white for $K \leq 2\pi R_o^{-1}$, conforms rather to the conventional large-area scaling law $Q_{o-}(\omega) = 2(\omega R_c / U_\infty)^{-2} \rho^2 \delta_*^3 U_\infty^3 G_-(\omega \delta_* / U_\infty)$, where δ_* is the TBL displacement thickness. The rate of decrease of flow noise with distance aft may be much less than would be inferred from the conventional scaling law.

DOME EFFECTIVENESS AND THE SCALING AND AREA
DEPENDENCE OF BOUNDARY-LAYER PRESSURE SPECTRA
VIEWED WITH REGARD TO CHARACTERISTIC WAVENUMBER
RANGES*

D. M. Chase
TRG, Incorporated
A Subsidiary of Control Data Corp.
Route 110
Melville, New York

In the design of sonar systems, achievement of optimum configurations, or positive control, for flow noise depends on adequately understanding its generation by pressure fluctuations associated with a turbulent boundary layer. In our efforts, we have to guard against overreliance on theoretical restatement of empirical observation, which we may extrapolate beyond its range of validity, and against use of overspecialized theoretical models, which outside some restricted domain may be groundless and are often unnecessary. In this paper we aim to emphasize certain facts and presumptions, mostly already recognized, and use a corresponding characterization of the pressure field to point out relations depending mainly on the grosser and more immediately relevant properties, with application both to flush-mounted and dome-shielded elements and arrays.

Wavenumber spectrum of pressure; frequency spectrum of average pressure on a large element

For turbulent flow on an infinite plane rigid boundary we introduce the wavenumber-frequency spectrum of pressure at a point on this boundary, $P(\bar{K}, \omega)$ [$\bar{K} = (K_1, K_2)$], and its integral over directions of \bar{K} in the plane,

$$(1) \quad I(K, \omega) = \int_0^{2\pi} d\theta P(\bar{K}, \omega).$$

* This work was sponsored by the Undersea Programs Branch of Office of Naval Research under contract Nonr 4385.

On a circular element of radius R_0 , the frequency spectrum of average pressure then is

$$(2) \quad Q_0(\omega) = \int_0^{\infty} dK K \left[2J_1(KR_0)/KR_0 \right]^2 I(K, \omega),$$

the area-averaging factor in brackets approaching unity as $R_0 \rightarrow 0$. The general character of the basic function I at fixed, relatively high frequency ($\omega \delta_* / U_{\infty} \gg 1$), together with the area-averaging factor (with added geometric factor K), is shown in Figure 1. The broad peak above $K = \omega / U_{\infty}$ corresponds to the well known wavenumber range of convection; i.e., boundary-layer eddies of frozen shape convected downstream at speed u generate pressure fluctuations of frequency ω only via the wavenumber component $K_1 = \omega / u$; hence, if the convection speed at no depth in the layer exceeds the asymptotic flow speed U_{∞} , only wavenumbers $K \geq K_1 \geq \omega / U_{\infty}$ are present. Below this peak lies a "tail" deriving from nonconvective effects, that is, decay and distortion of eddies in the shear flow.

$I(K, \omega)$ in the convective range is susceptible to estimation by means of semiempirical models of the convected velocity field, as by Kraichnan [1] and many others. In the nonconvective tail, I is less accessible to theory. But in average-pressure spectra on elements with $\omega R_0 / U_{\infty} \gg 1$ this range is strongly weighted. In fact, we reasonably approximate Q_0 as a sum of contributions Q_{0-} from a low-wavenumber interval where the reduction factor due to averaging is not small and Q_{0+} from the high-wavenumber interval where I has its convective peak:

$$(3) \quad Q_0(\omega) \approx Q_{0-}(\omega) + Q_{0+}(\omega) \quad (\omega R_0 / U_{\infty} \gg 1),$$

$$(4) \quad Q_{0-}(\omega) = \int_0^{mR_0^{-1}} dK K \left[2J_1(KR_0)/KR_0 \right]^2 I(K, \omega),$$

$$(5) \quad Q_{0+}(\omega) = (4/\pi) R_0^{-3} \int_{\omega/U_{\infty}}^{\infty} dK K^{-2} I(K, \omega)$$

where m is a fixed number somewhat large relative to unity and the range $mR_0^{-1} < K < \omega / U_{\infty}$ is neglected. We

have averaged over oscillations of J_1 in Q_{0+} , but the dependence on R_0 as R_0^{-3} is obtained also without this approximation.

The low-wavenumber part, Q_{0-} , can decrease less rapidly with increasing R_0 than as R_0^{-3} . For example, suppose that over all $K < mR_0^{-1}$, except for a negligible range of K (near $K = 0$),

$$(6) \quad I(K, \omega) \propto K^n, \quad (n \geq 0)$$

We then find immediately that

$$(7) \quad Q_{0-} \propto \begin{cases} R_0^{-(2+n)} & \text{if } 0 \leq n < 1, \\ R_0^{-3} & \text{if } 1 < n. \end{cases}$$

Now, it is commonly accepted on the basis of direct and indirect measurement that for a large element (possibly with other restrictions) $Q_0 \propto R_0^{-2}$ (e.g. see Ref. [2]).

If so, we would conclude that $I(K, \omega)$ varies modestly over most of the range $0 < K < mR_0^{-1}$, and obtain from (4)

$$(8) \quad Q_{0-} \approx 2R_0^{-2} I(\sim R_0^{-1}, \omega),$$

where $I(\sim R_0^{-1}, \omega)$ denotes a suitable average but is sensibly independent of R_0 . Nevertheless, we may not necessarily identify $I(\sim R_0^{-1}, \omega)$ with $I(0, \omega)$, which is proportional to the area scale; i.e. the effective area scale for the averaging area πR_0^2 may be larger than the true area scale pertinent to an unbounded area.*

*The area scale, denoting $2\pi I(0, \omega)/P(\omega)$ with

$P(\omega) = \int dK K I(K, \omega)$, would be a measure of the area over which the pressure field is correlated only if $I(K, \omega)$ were fairly flat out to some wavenumber cutoff, which would then be roughly twice the effective correlation radius. For the pressure field in question, such is not at all the case.

At wavenumber K of the order of the sound wave-number (ω/c) it appears quite possible that the spectrum $I(K, \omega)$ has a local peak (see Figure 1). In particular, if one expresses I formally as an integral over the source field of velocity derivatives as in a recent paper by Flowce Williams [3], and regards the source field as the same as for incompressible flow, one obtains a divergent expression at $K = \omega/c$. The turbulent velocity and the acoustic particle velocity in this spectral domain thus seem essentially coupled. If extant, this peak produces a "radiative" contribution to the average-pressure spectrum in (4) that, for $\omega R_0/c \lesssim 1$ (R_0 small compared to the sound wave length) is independent of R_0 .

Acceptance of (8) and inclusion of this possible radiation contribution, together with (5), yields a spectrum depending on R_0 as

$$(9) \quad Q_0(\omega) = A(\omega)R_0^{-2} + C(\omega)R_0^{-3} + B(\omega)$$

$$(\omega R_0/U_\infty \gg 1, \omega R_0/c \lesssim 1).$$

Noise reduction by a fluid dome

We proceed to consider a dome-shielded element. We model the dome as a fluid slab of thickness L and later, where convenient, will regard it nominally as circular of radius a (see Figure 2). We refer to a in any case as a measure of its lateral extent. Here we imagine a dome cover of negligible impedance, therefore calling the slab a fluid dome. This fluid sheath serves likewise as the prototype for a (fairly thin) elastic-solid sheath, provided the transverse sound velocity c_t satisfies

$c_t \gg U_\infty$; c_t is roughly identified with c as used here. We neglect the effect of boundary motion on the excitation spectrum $I(K, \omega)$.

Contributions to the average-pressure spectrum $Q(\omega, -L)$ on an element of radius r_0 in the inner surface may be distinguished as due to low or high wavenumbers in the excitation spectrum $I(K, \omega)$:

$$(10) \quad Q(\omega, -L) = Q_-(\omega, -L) + Q_+(\omega, -L).$$

We consider first the former. If the lateral size is great enough, namely if

$$(11) \quad (\omega L/c) (\omega a/c)^{-1/2} \ll 1,$$

we find we may regard the fluid slab as infinite in computing this part. Thus, we have

$$(12) \quad Q_-(\omega, -L) \approx \int_0^{mR_0^{-1}} dK K \left[2J_1(KR_0)/KR_0 \right]^2 I(K, \omega) |\Gamma(K, \omega, -L)|^2,$$

which is the same as (4) for a flush element except for the factor $|\Gamma|^2$, where Γ denotes the interior acoustic-response coefficient. For a rigid inner surface $|\Gamma|^2$ is given for radiative and attenuative wavenumber ranges by

$$(13) \quad |\Gamma(K, \omega, -L)|^2 = \begin{cases} 1 & \text{for } K < \omega/c \\ \exp[-2(K^2 - \omega^2/c^2)^{1/2} L] & \text{for } K > \omega/c, \end{cases}$$

as illustrated in Figure 1. To obtain a tentative, indicative result, we assume that $I(K, \omega)$ varies only modestly over most of the interval $0 < K < K_m^*$, where K_m is the smaller of mR_0^{-1} and $2R_e^{-1}$, with R_e defined by

$$(14) \quad R_e^{-2} = (1/4) \left[(\omega/c)^2 + (1/2)L^{-2} \right].$$

We then find

* If $I(k, \omega)$ has a peak at $K \approx \omega/c$, the additional contribution to $Q_-(\omega, -L)$, for $\omega a/c \gg \pi$, will be the same as the corresponding contribution to $Q_0(\omega)$ for a flush element of the same size [e.g., $B(\omega)$ in Eq. (9)], that is, unaffected by the dome independently of depth.

$$(15) \quad Q_-(\omega, -L) \approx \begin{cases} 2r_0^{-2} I(\sim r_0^{-1}, \omega) \approx Q_{0-}(\omega, r_0) & \text{for } R_e \lesssim r_0 \gg \omega/U_\infty \\ 2R_0^{-2} I(\sim R_0^{-1}, \omega) \approx H(R_0/R_e)^2 Q_{0-}(\omega, R_0) & \text{for } R_e \gtrsim r_0, \end{cases}$$

where $H = I(\sim R_e^{-1}, \omega) / I(\sim R_0^{-1}, \omega) (\lesssim 1)$ with $I(\sim R_e^{-1}, \omega)$ a suitably defined average of I in the interval $0 < K \lesssim 2R_e^{-1}$. The element radius is here included as an explicit argument in the spectrum Q_{0-} for a flush element. In the form given for $R_e \gtrsim r_0$, the radius R_0 refers to an arbitrary large ($R_0 \gg U_\infty/\omega$), flush-mounted comparison element.

R_e measures the spatial extent of correlation of interior pressure, and for element radius $r_0 \lesssim R_e$ the average-pressure spectrum (if $H \sim 1$) is roughly the same as for a flush element of radius R_e . The spectrum is seen to be lower than for a flush element of radius $R_0 (\gg U_\infty/\omega)$ only for sound wave lengths $\gtrsim 4R_0$, and then only for dome thickness $> R_0/2$.

On the basis of Eq. (15), referring still to the low-wavenumber contributions, we may likewise compare arrays of flush and of sheathed elements. Optimum configurations for fixed active area depend on whether the spectrum $I(K, \omega)$ declines substantially at small wavenumbers $K \sim \Lambda_T^{-1/2}$, where $\Lambda_T^{1/2}$ is a linear dimension of the array (or of the array within a single dome section, if the dome is partitioned). Thus, if $I(\sim \Lambda_T^{-1/2}, \omega) \ll I(\sim R_0^{-1}, \omega)$ in the case of a flush array, or if $I(\sim \Lambda_T^{-1/2}, \omega) \ll I(\sim R_0^{-1}, \omega)$ in the case of a sheathed array, reduction in the noise pressure spectrum averaged over active area could be achieved by packing the array as tightly as possible, subject to other constraints, to take advantage of coherent cancellation by neighboring elements.

On the contrary assumption that I does not thus decline or that tight packing is excluded, for an array of N flush elements of radius R_0 ($\gg U_{\infty}/\omega$) the spectrum $Q_{0-}^A(\omega)$ of pressure averaged over the total active area A is independent of R_0 and varies inversely as A :

$$(16) \quad Q_{0-}^A(\omega) \approx Q_{0-}(\omega, R_0)/N \approx 2\pi A^{-1} I(\sim R_0^{-1}, \omega).$$

On the same assumption, for a sheathed array of fixed active area and maximum total (active plus dead) area, the spectrum averaged over active area instead has a minimum achieved by packing the array as loosely as possible and choosing the smallest permissible element size.

For such a sheathed array, if the total-to-active area ratio exceeds 4 and $L > 0.7 r_0$ (with $H \sim 1$), there is a maximum frequency ω_c below which the noise-reduction

factor relative to a flush array is 6 db or more.* This is shown as a function of depth L for element diameters 1.2 in. and 4.8 in. in Figure 3. At $L = r_0$, with the sound velocity c for water, we have $\omega_c/2\pi = 0.7 c/r_0 = 13 \text{ kc}/r_0$ with diameter $2r_0$ in inches.

As for the contribution $Q_+(\omega, -L)$ from high wave numbers [Eq. (10)], two principal contributions may be distinguished according to the wavenumber range of the response modes (n) of the dome; for given excitation wave number K, these are (1) a "direct" part Q_+^{∞} due to modes with $K_n \approx K$ and (2) an "overlap" part Q_+^P due to modes with $K_n \lesssim (\omega^2/c^2 + L^{-2})^{1/2}$ such that acoustic waves are not highly attenuated at the inner dome surface:

$$(17) \quad Q_+(\omega, -L) \approx Q_+^{\infty}(\omega, -L) + Q_+^P(\omega, -L).$$

The former remains even in the limit of a laterally infinite dome ($a \rightarrow \infty$) and is roughly related to the high-wavenumber part of the spectrum $Q_{0+}(\omega, r_0)$ for a flush element of the same radius r_0 by

$$(18) \quad Q_+^{\infty}(\omega, -L) \sim \exp(-2\alpha L/U_{\infty}) Q_{0+}(\omega, r_0).$$

This quantity is effectively obliterated by taking $L \gtrsim 4U_{\infty}/\omega$, say, e.g., at $\omega/2\pi = 3 \text{ kc}$ and $U_{\infty} = 20 \text{ kt}$, by taking $L \gtrsim 0.1 \text{ in.}$

The other part, Q_+^P , depends explicitly on the assumed geometry and lateral boundary conditions, and also is not generally and simply expressible. In the model considered, with typical boundary conditions, however, in a certain restricted parameter domain based on lateral largeness of the dome in units of wave lengths, namely where conditions (11) and

* If the elements are at depth L in an interior medium of effectively infinite depth rather than mounted in a rigid inner surface, there is a reduction by an additional 6 db.

$$(19) \quad (\omega L/c)^{-1} (\omega a/c)^{-1/2} \ll 1$$

apply, we derive a limiting form given roughly, for $\omega R_0/c \lesssim 1$, by

$$(20) \quad Q_+^P(\omega, -L) \sim (\omega L/c)^2 F(\omega a/c) (R_0/a)^3 Q_{0+}(\omega, R_0),$$

where F denotes a certain positive periodic function with period π and order of magnitude unity [5]. In view of conditions (11) and (19), we may consider the factor

$(\omega L/c)^2 \sim 1$. Eq. (20) relates Q_+^P to the spectrum $Q_{0+}(\omega, R_0)$ for a flush element of arbitrary radius $R_0 (\gg U_\infty/\omega)$. Q_+^P is seen to be of the order of the high wavenumber part of the spectrum for a flush element having radius equal to the dome radius a and varies as a^{-3} . This role of the dome size as an averaging radius probably persists more generally than (20).

Hence if high wavenumbers ($K \gtrsim \omega/U_\infty$) dominated the spectrum (i.e. if $Q_+ \gtrsim Q_-$), a rather thin fluid (or solid) sheath of large lateral extent would suffice to reduce flow noise greatly. The measured area dependence for large flush transducers, $(\omega R_0/U_\infty \gg 1)$, however, suggested that the low- K component there prevails, i.e. $Q_{0+} \lesssim Q_{0-}$. If so, it follows from the previous relations between $Q_{0+}(\omega, R_0)$ and $Q_+(\omega, -L)$, respectively, that $Q_-(\omega, -L) \gtrsim Q_+(\omega, -L)$; hence, the earlier discussion of low-wavenumber contributions applies roughly to the total spectrum and, in particular, a fluid sheath substantially reduces noise only if its thickness is roughly at least half the element diameter. Experimentally, measurement of the noise spectrum for several different sheath thicknesses, or different element recessions within a fluid dome, appears to afford a useful method for better establishing the wavenumber spectrum of boundary-layer pressure fluctuations.

Scaling of boundary-layer pressure spectra

We turn now briefly from the effect of domain to the scaling of boundary-layer pressure spectra with parameters of the flow. This question is rudimentary to understanding the structure and possible alteration of the pressure field and to predicting the dependence of flow noise on distance aft of the bow in a parameter regime beyond available measurements.

With reference first to the convective (high-wavenumber) contribution to spectra, from the usual relation between boundary pressure and velocity sources, contributions are attenuated exponentially with source depth (y) in the boundary layer and with parallel wavenumber (K) of the source component (i.e., $\propto e^{-2Ky}$). In consequence, at sufficiently high frequencies, since $K > \omega/U_\infty$, the predominant velocity sources are those located in the transition layer just outside the viscous sublayer, i.e., at a distance characterized as a multiple of v/v_* , the thickness of the sublayer being $\sim 6v/v_*$, where v is kinematic viscosity and v_* the friction velocity.* Likewise, the mean velocity in this region is characterized

Thus, in Fig. 1 the spectrum for $K > K' (\omega/U_\infty)$ is due mainly to sources at $y \lesssim K'^{-1}$. Even on assumption of pure local convection [$K_1 = \omega/u(y)$], each y contributes up to values K somewhat greater than $\omega/u(y)$ by virtue of spectral components with $K_3 \neq 0$. Hence, for example, the transition layer is indicated in Fig. 1 as contributing in a range of K that overlaps the range for the viscous sublayer. (The transition layer may be regarded as extending from depth $y = 6v/v_$ to depth equal to the geometric mean of δ_* and $6v/v_*$.) The rough upper bound $v_*/6v + \omega/6v_*$ shown on K is established as follows. At the edge of the viscous sublayer (and within) we have $\exp[-2\omega y/u(y)] = \exp(-2\omega v/v_*^2)$; with $K_1 = \omega/u(y)$, this represents $\exp(-2Ky)$ for $K_3 = 0$; $\exp(-2Ky)$ at this depth is then smaller by at least a factor e^{-2} for such K_3 that $K > v_*/6v + \omega/6v_*$.

as a multiple of v_* (which, however, at high Reynolds number is nearly proportional to U_∞). Thus, displacement thickness δ_* and asymptotic flow velocity U_∞ , the parameters pertaining to the boundary layer as a whole, are not directly involved.* From the parameters v and v_* of the inner layer alone we can form a dimensionless frequency variable $\omega v/v_*^2$, wavenumber variable Kv/v_* , and wavenumber-frequency spectral density of pressure

$$(21) \quad I(K, \omega) = \rho^2 v^3 G_+(Kv/v_*, \omega v/v_*^2) \quad (K \gtrsim \omega/U_\infty, \omega v/v_*^2 \gtrsim 0.1),$$

where the given restriction to high frequency and to convective wavenumbers roughly insure the predominance of the inner layer and G_+ signifies a function of the

indicated dimensionless arguments. In the frequency spectrum $P(\omega)$ of point pressure we distinguish once more the high-wavenumber, convective part $P_+(\omega)$ and the remaining part $P_-(\omega)$:

$$(22) \quad P(\omega) = P_-(\omega) + P_+(\omega)$$

* Admitting that at high frequency the significant velocity sources for the convective contribution are those near the sublayer, one might still contend that these sources are associated in substantial degree with eddies having one or more spatial scales large of the order of δ_* , and hence that δ_* may still enter the pressure scaling, contrary to forms (21) and (24). Explicit consideration indicates that this supposition is likely untenable. For example, if one crudely assumed an isotropic velocity spectrum with scale $\sim \delta_*$, one would infer, for $\omega \delta_*/U_\infty \gg 1$, that the pertinent wavenumber range for convected sources lies in the inertial subrange, where the Kolmogorov spectrum would hold. The large-scale properties then would enter the derived pressure spectrum only via the energy dissipation rate ϵ . But in the constant-stress layer both experiment and the usual law of the wall yield $\epsilon \approx v_*^3/0.42y$, whence the eddy scale, contrary to assumption, would have to be $\sim 0.4y$, not δ_* . Examples more accordant with the actual anisotropic boundary-layer velocity field may also be examined.

$$(23) P_-(\omega) = \int_0^{\omega/U_\infty} dK KI(K, \omega), \quad P_+(\omega) = \int_{\omega/U_\infty}^{\infty} dK KI(K, \omega).$$

From (21) we then infer for high frequency the "inner" scaling form

$$(24) \quad P_+(\omega) = \rho^2 v_*^2 H_+(\omega v_*^{-2}) \quad (\omega v_*^{-2} \gtrsim 0.1).$$

Likewise, for a large element ($\omega R_\infty / U_\infty \gg 1$) we infer for the average-pressure spectrum of Eq. (5)*

$$(25) \quad Q_{O+}(\omega) = (\omega R_\infty / v_*)^{-3} \rho^2 v_*^2 L_+(\omega v_*^{-2}) \\ (\omega v_*^{-2} \gtrsim 0.1, \omega R_\infty / U_\infty \gg 1).$$

In some other domain of frequency and wave number, the pertinent length and velocity scales may well be those characteristic of the full boundary layer, δ_* and U_∞ .

This presumption is likely to be valid at least in the large-scale domain where $K \lesssim \delta_*^{-1}$ (which corresponds entirely to a nonconvective part of the spectrum if $\omega \delta_* / U_\infty > 1$). In such a domain, contrary to (21) we have

$$(26) \quad I(K, \omega) = \rho^2 \delta_*^3 U_\infty^3 G_-(K \delta_*, \omega \delta_* / U_\infty) \quad (K \lesssim \delta_*^{-1}).$$

In the low-frequency range where $\omega \delta_* / U_\infty \lesssim 1$ we infer from (26) the "outer" scaling form

$$(27) \quad P_-(\omega) = \rho^2 \delta_* U_\infty^3 H_-(\omega \delta_* / U_\infty) \quad (\omega \delta_* / U_\infty \lesssim 1).$$

In fact, if (26) holds for $K < M \delta_*^{-1}$, where M may prove somewhat larger than unity, then for $\omega \delta_* / U_\infty \lesssim M/5$ we can infer that the entire spectrum $P(\omega)$ also has this outer form, since $I(K, \omega)$ is presumably small for $K > [\delta_*^{-2} + (5\omega/U_\infty)^2]^{1/2}$ (cf. Figure 1):

* Here U_∞ in the lower limit in Eq. (5) is adequately regarded as a multiple of v_* .

$$(28) \quad P(\omega) = \rho^2 \delta_* U_\infty^3 H(\omega \delta_* / U_\infty) \quad (\omega \delta_* / U_\infty \lesssim 1).$$

Analogously to (28), under similar conditions we infer also from (26) and (5) (or the exact form of the latter) a form for the spectrum $Q_0(\omega)$ corresponding to an arbitrary averaging radius R_0 ?

$$(29) \quad Q_0(\omega) = (\omega R_0 / U_\infty)^{-2} \rho^2 \delta_* U_\infty^3 N(\delta_* / R_0, \omega \delta_* / U_\infty) \\ (\omega \delta_* / U_\infty \lesssim 1).$$

If, as considered earlier, $I(K, \omega)$ varies little for most $K < \pi R_0^{-1}$, which for $\omega \delta_* / U_\infty \lesssim 1$ can be true only for a large element such that $R_0 \gtrsim (\pi/M) \delta_*$, Eq. (29) assumes the simpler form

$$(30) \quad Q_0(\omega) = 2 (\omega R_0 / U_\infty)^{-2} \rho^2 \delta_* U_\infty^3 \hat{G}_-(\omega \delta_* / U_\infty) \\ (\omega \delta_* / U_\infty \lesssim 1, R_0 \gtrsim \delta_*),$$

where \hat{G}_- is identified as a suitable average over $K \delta_*$ of the function G_- in Eq. (26). Scaling forms (28) and (30) are those commonly used for correlation and extrapolation of measured data.

In the high-frequency range where $\omega \delta_* / U_\infty \gtrsim 1$ we cannot infer for $P_-(\omega)$ either the outer form (27) or the inner form (24) without knowledge of the scaling of $I(K, \omega)$ for $\delta_*^{-1} \lesssim K \lesssim \omega / U_\infty$. Nevertheless, for $R_0 \gtrsim (\pi/M) \delta_*$ we can infer from (26) that Q_{0-} (not Q_0) has the outer form (29) or, if $I(K, \omega)$ varies little for $0 < K < \pi R_0^{-1}$, the simplified form (30). If also $\omega \nu / v_*^2 \gtrsim 0.1$ (which implies $\omega \delta_* / U_\infty \gg 1$ at Reynolds numbers of concern), form (25) for Q_{0+} and (30) for Q_{0-} yield

$$(31) \quad Q_0(\omega) = 2 (\omega R_0 / U_\infty)^{-2} \rho^2 \delta_* U_\infty^3 \hat{G}_-(\omega \delta_* / U_\infty) \\ + (\omega R_0 / v_*)^{-3} \rho^2 \nu v_*^2 L_+(\omega \nu / v_*^2) \quad (R_0 \gtrsim \delta_*, \omega \nu / v_*^2 \gtrsim 0.1).$$

From these rudimentary considerations, we remain uncertain how P_- scales when $\omega \delta_* / U_\infty \gtrsim 1$ and whether P_- or P_+ predominates in $P(\omega)$ at these frequencies; hence we cannot predict the scaling of point pressure $P(\omega)$ at high frequency. The conventional dimensionless plot of measured data is based on the outer scaling law (28). We know that diverse data in fact coalesce rather well on such a plot. For example, Figure 4 shows this for some wind-tunnel measurements by Willmarth and Wooldridge [6] and by Bull [7]. We disregard the ascissa range $10 \log(\omega \delta_* / U_\infty) \gtrsim 7$, since the finite-area effect, which is ignored in these plots, is substantial there. At the lower frequencies the outer law agrees well with experiment, as expected. Now, in Figure 5, we view the same data on the dimensionless plot based instead on the inner scaling law (24). Since this law is well founded (even for P_+) only where $10 \log(\omega v_*^2) \gtrsim -10$ and the area effect here is substantial for $10 \log(\omega v_*^2) \gtrsim -9$, we should consider only a limited neighborhood near -10 . At these frequencies, the data shown permit no clear choice between the laws, but appear somewhat to favor the inner law.

The question of pressure scaling has immediate practical consequence in the dependence of flow noise on distance aft. Referring now to a large transducer, suppose the spectrum $Q_o(\omega)$ is correctly given at high frequency by (31). If in some domain $Q_o(\omega)$ is observed to vary with frequency as $\omega^{-(n+2)}$ for some n , then, on assumption that Q_{o-} there prevails, we should have*

$$(32) \quad Q_o(\omega) \sim Q_{o-}(\omega) \propto R_o^{-2} U_\infty^{4.84 + 1.16n} x^{-0.84(1-n)},$$

where x denotes distance aft; whereas, on assumption that Q_{o+} prevails, we should have

$$(33) \quad Q_o(\omega) \sim Q_{o+}(\omega) \propto R_o^{-3} U_\infty^{2.80 + 1.87n} x^{-0.20 - 0.13n}.$$

* Appropriate to the regime of very high Reynolds number we take $v_* \propto x^{-0.066} U_\infty^{0.93}$, $\delta_* \propto U_\infty^{-0.16} x^{0.84}$.

For typical observed high-frequency spectra, we have roughly $n \sim 2$; with this value Eqs. (32) and (33) yield respectively the x -dependences $Q \propto x^{-0.84}$, $x^{-0.46}$ *

Even if Q_{0-} prevails in the domain of available measurements, the possibility exists that for much larger x (and the same upper limit on ω/U_∞) Q_{0+} will become dominant, primarily because the argument $\omega \delta_* / U_\infty$ increases more rapidly with x (as $x^{0.84}$) than does $\omega v_* / v_*^2$ (as $x^{0.13}$). In any event, the scaling of pressure with boundary-layer parameters cannot be regarded as well established over the entire range of interest, and, in particular, the decrease of flow noise with distance aft may be much less than would be inferred from the conventional scaling law.

Conclusion

In summary, in the wavenumber spectrum of boundary layer pressure at given frequency we usefully distinguish low- and high-wavenumber ranges, the latter corresponding to possible generation by a convected eddy field. In the frequency spectrum of average pressure on a large flush element, the high-wavenumber component varies as R_0^{-3} , and the low probably more as R_0^{-2} . Acceptance of experimental indications that the total varies roughly as R_0^{-2} implies dominance of the low-wavenumber part.

With regard to a dome-shielded or sheathed element, the high-wavenumber contribution to the pressure spectrum is reduced relative to that for flush mounting much as though averaged over the lateral area of the dome section, provided the sheath thickness exceeds a small (frequency-

* In some range where R_0 / δ_* is small and $\omega R_0 / U_\infty$ not extremely larger than unity, $Q_{0-}(\omega)$ might have the form (25) with exponent ~ -2 instead of -3 on $\omega R_0 / v_*$, in place of the form (28), leading, for $Q_{0-} \propto \omega^{-(n+2)}$, to $Q_{0-} \propto R_0^{-2} U_\infty^{3.74 + 1.87n} x^{-0.26 - 0.13n}$.

dependent) value. The low-wavenumber contribution is reduced rather as though averaged over an area of radius given roughly by the smaller of one-third the sound wave length or three times the sheath thickness. Dominance of the low-wavenumber part in the spectrum on a large flush element implies its dominance on a shielded element. In such event, substantial reduction in flow noise averaged over the active area of an array of elements probably can be effected by a sheath or dome only if the elements are loosely packed and the dome thickness is not less than the element radius r_0 ; reduction then extends up to a certain maximum frequency ($\sim 0.7c/2\pi r_0$ cps).

The low- and high-wavenumber parts of the wavenumber-frequency spectrum of boundary-layer pressure at high frequency scale with the flow parameters in different, partially discernible ways. The high-wavenumber part of the point pressure spectrum at high frequency is expected to scale with length and velocity parameters characteristic of the inner boundary layer, and the entire spectrum may well also scale this way, rather than with parameters used in conventional dimensionless plots, which are appropriate at lower frequency. The inferred dependence of average-pressure spectra on distance aft at high frequency differs according to the relative contributions of low and high wavenumbers; the rate of decline of high-frequency flow noise with distance aft may be substantially less than suggested by the conventional scaling law.

References

1. R.H. Kraichnan, J. Acous. Soc. Am. 28, 378 (1956).
2. G.M. Corcos, J. Acoust. Soc. Am. 35, 192 (1963).
3. J.E. Ffowcs Williams, J. Fluid Mech. 22, 507 (1965).
4. G.J. Franz, JUA (USN) 12, 5 (1962) (Confidential).
5. D.M. Chase, "Flow Noise Transmitted Through Domes or Modified by Non-Rigid Boundaries," TRG-011-TN-65-1, under ONR contract Nonr 4385(00), December, 1965.
6. W.W. Willmarth and C.E. Wooldridge, "Measurements of the Fluctuating Pressure at the Wall Beneath a Thick Turbulent Boundary Layer," U. of Michigan, Dept. of Aero. and Astro. Engin., Technical Rept. 02920-1-T (April, 1962).

7. M.K. Bull, AGARD (NATO), Report 455 (April, 1963).

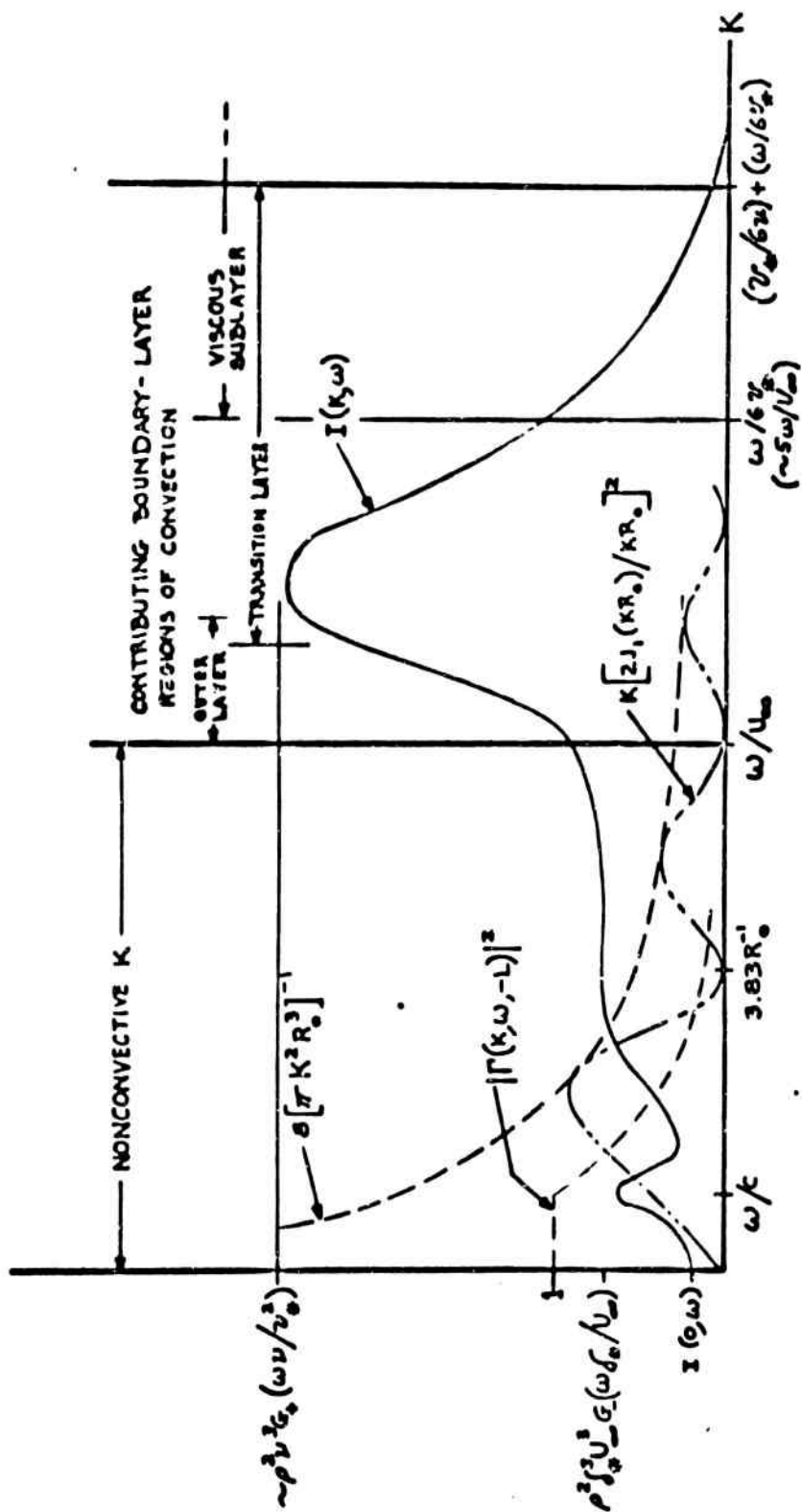


Figure 1. Wavenumber spectrum of boundary-layer pressure at high frequency $I(K, \omega)$; averaging-weighting factor $K [2J_1(kR_0)/kR_0]^2$ for circular area πR_0^2 ; interior acoustic-response function $|\Gamma(k, \omega, -L)|^2$.

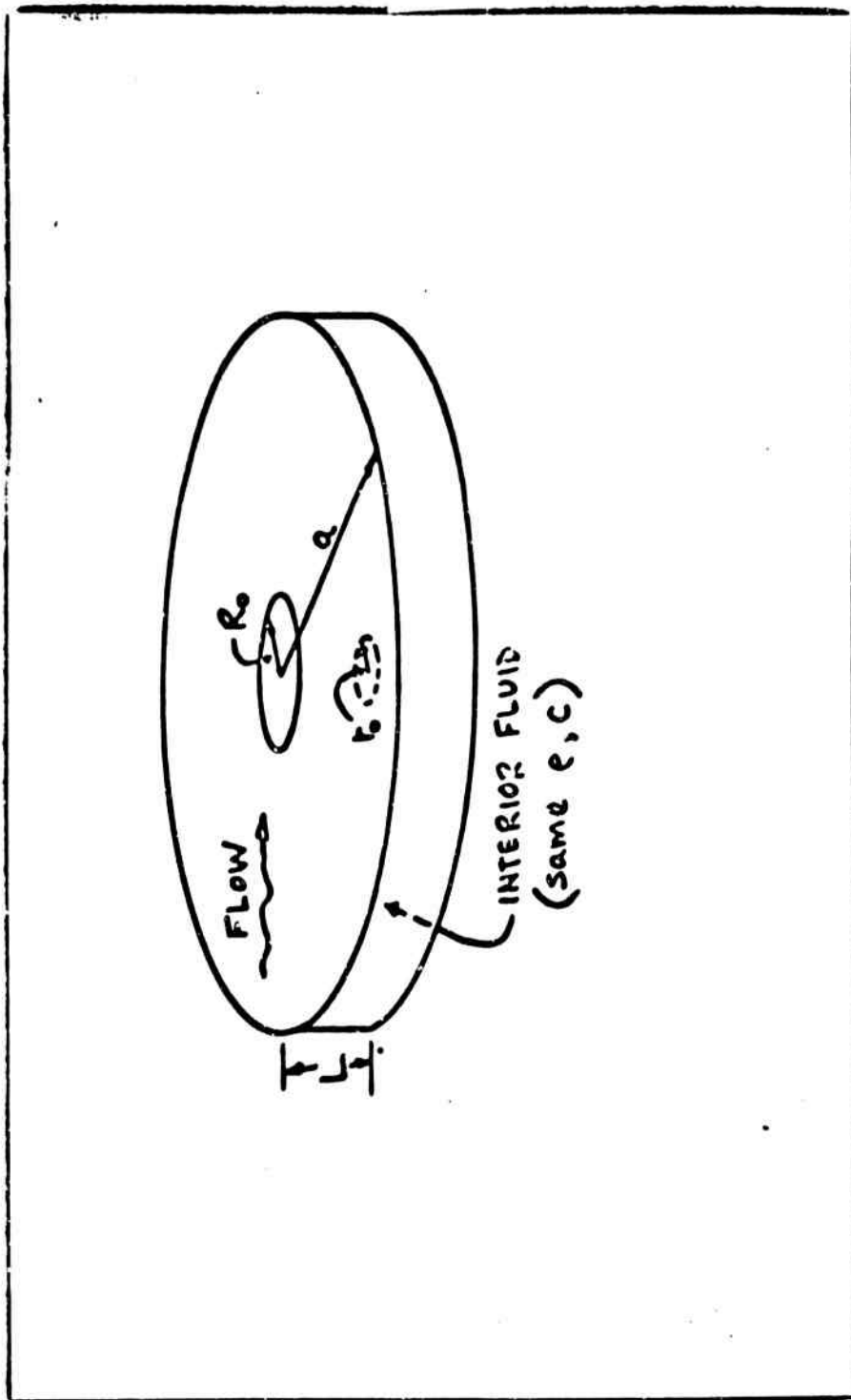
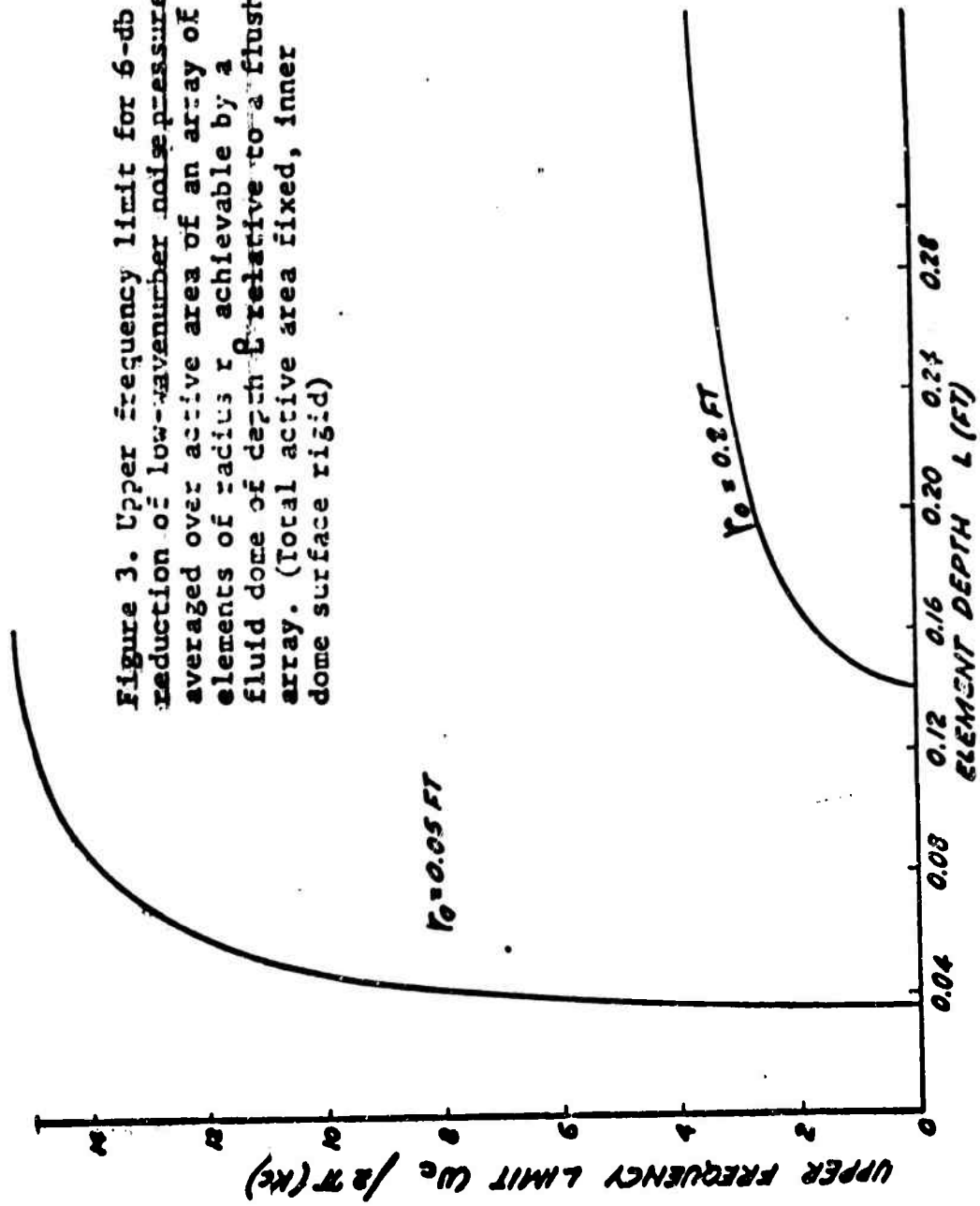


Figure 2. Fluid dome or sheath.

Figure 3. Upper frequency limit for 6-db reduction of low-wavenumber noise pressure averaged over active area of an array of elements of radius r achievable by a fluid dome of depth l relative to a flush array. (Total active area fixed, inner dome surface rigid)



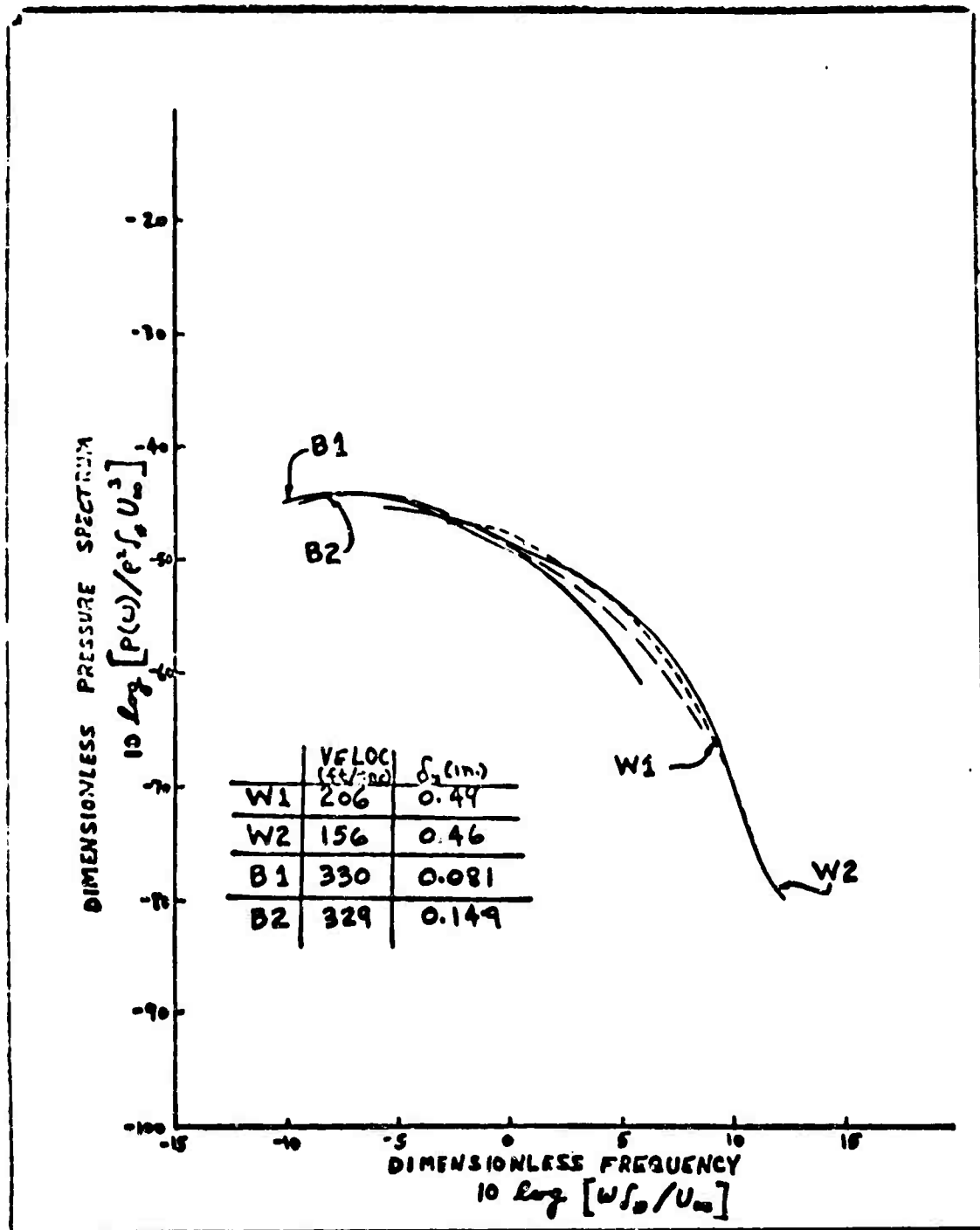


Figure 4. Experimental boundary-layer pressure spectra plotted via (conventional) dimensionless variables for outer scaling form. (W1,W2: Ref.[6], B1,B2: Ref.[7])

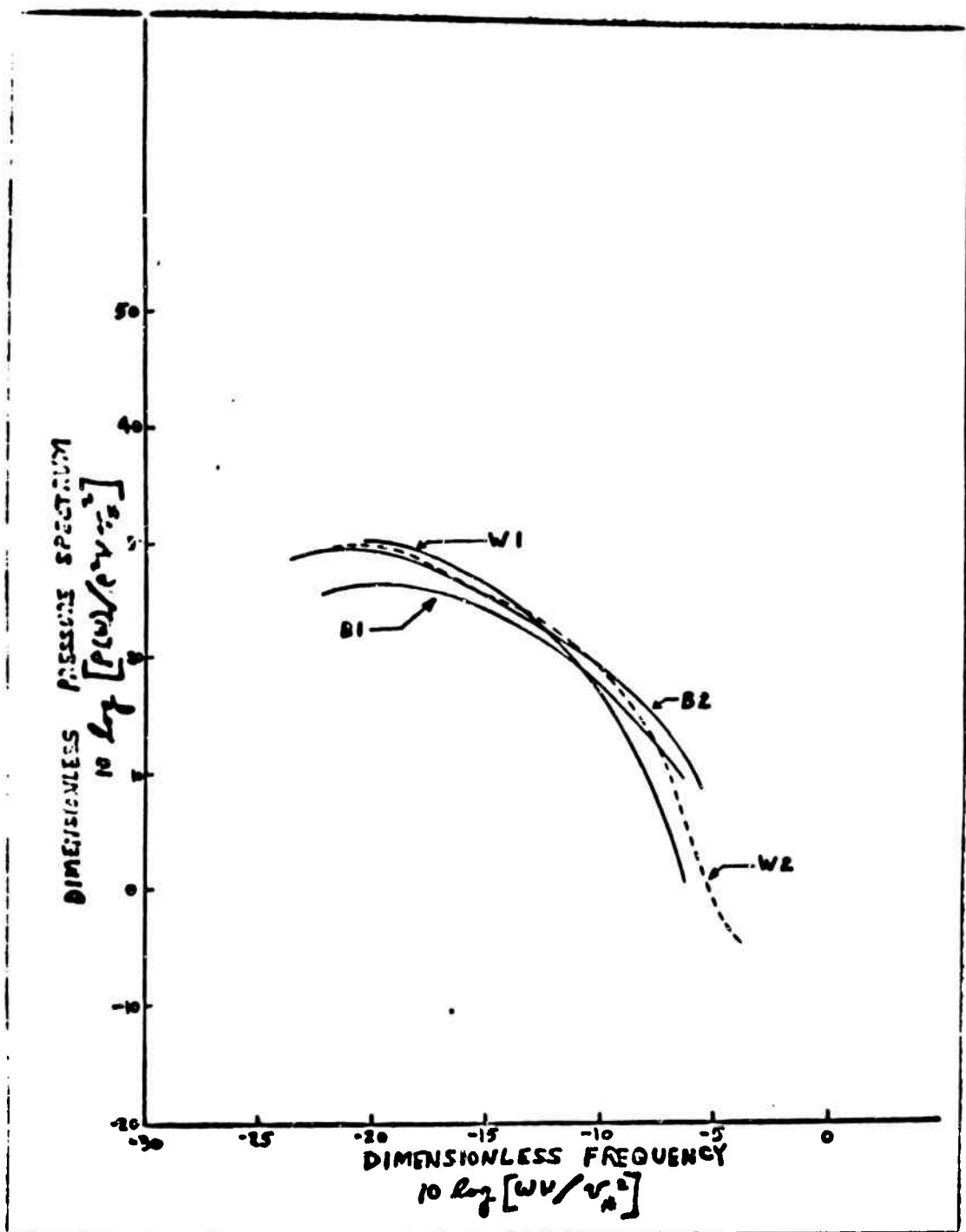


Figure 5. Experimental boundary-layer pressure spectra plotted via dimensionless variables for inner scaling form. (Data same as in Fig. 4)

Contract No. Nonr 4385(00)

	<u>No. Of Copies</u>		<u>No. Of Copies</u>
Office of the Secretary of Defense Director of Defense Research and Engineering Washington, D.C. 20301 Attn: Asst. Dir. Sea Warfare Systems	1	Chief of Naval Research Department of the Navy Washington, D.C. 20360 Code 406T (1 cy) Code 466 (2 cys) Code 468 (1 cy) Code 408 (1 cy) Code 421 (1 cy)	6
Assistant Secretary of the Navy (Research and Development) Department of the Navy Washington, D.C. 20350	1	University of Michigan Cooley Electronics Laboratory Ann Arbor, Michigan 48105 Attn: Mr. R.M. Grant	1
Director Systems Analysis Staff Building 90-213 Naval Ordnance Laboratory, White Oak Silver Spring, Maryland 20910	1	Director Weapons Systems Evaluation Group Department of Defense Washington, D.C. 20350	1
Director Marine Physical Laboratory Scripps Institution of Oceanography San Diego, California 92152	1	Director Woods Hole Oceanographic Institution Woods Hole, Massachusetts 02543	1
Director Ordnance Research Laboratory Pennsylvania State University University Park, Pennsylvania 16801	1	Director University of Texas Defense Research Laboratory P.O. Box 8029 Austin, Texas 78712	1
Commanding Officer and Director Navy Electronics Laboratory San Diego, California 92152 Code 3060	2	Director, Special Projects Office Department of the Navy Washington, D.C. 20360 SP 20	1
Director Defense Documentation Center Cameron Station Alexandria, Virginia 22314	20	Executive Director Committee on Undersea Warfare National Academy of Sciences 2101 Constitution Avenue, N.W. Washington, D.C. 20418	1
Director of Naval Warfare Analyses Institute of Naval Studies 545 Technology Square Cambridge, Massachusetts 02139	1	President Institute for Defense Analyses 400 Army Navy Drive Arlington, Virginia 22202	1
Commanding Officer and Director Navy Underwater Sound Laboratory Fort Trumbull New London, Connecticut 06321 Code 960 900 905 910 930 (1 cy each)	6	Commanding Officer and Director Naval Ship Research and Development Center Washington, D.C. 20007 Code 940 920	2
Commanding Officer and Director Navy Marine Engineering Laboratory Annapolis, Maryland 21402	1	Commanding Officer and Director Navy Mine Defense Laboratory Panama City, Florida 32502	2
Commander Naval Ordnance Laboratory White Oak Silver Spring, Maryland 20910 LE Div (1 cy) RA Div (1 cy)	2	Commander Naval Ordnance Test Station China Lake, California 93557	1
Officer in Charge Pasadena Annex Naval Ordnance Test Station China Lake 3203 E. Foothill Blvd. Pasadena, California 91107	1	Director Naval Research Laboratory Washington, D.C. 20390 Code 2027 5550	7
Superintendent Naval Postgraduate School Monterey, California 93940 Attn: Librarian	1	Director Navy Underwater Sound Reference Division Navy Research Laboratory P.O. Box 8337 Orlando, Florida 32806	2

contribution due to compressibility ($K \lesssim \omega/c$, $c =$ sound speed), for $\omega R_0/c \lesssim 1$, will be independent of R_0 . In the average-pressure spectrum on an area separated from the flow by a fluid layer of depth L , the high-wavenumber contribution is indicated to be reduced relative to an equal flush area much as though averaged not over the actual area πR_0^2 but over the entire lateral area of the layer face; in the limit of a lateral infinite layer, a residual reduction factor $\sim \exp(-2\omega L/U_\infty)$ instead applies. The low-wavenumber contribution is reduced rather as though averaged over an area πR_e^2 (if $R_e \gtrsim R_0$) where $R_e^{-2} = (1/4)[(\omega/c)^2 + (1/2)L^{-2}]$. With reference to noise reduction for an array of shielded elements, the effect of the increased correlation distance is also considered.

Regarding the scaling of TBL pressure on a flush area in the high-frequency range $\omega v/v_*^2 \gtrsim 0.1$, the probable length scale for the high-wavenumber part is the viscous-sublayer parameter v/v_* . If this contribution predominates in the point-pressure spectrum $P(\omega)$, the scaling law is $P(\omega) = \rho^2 v v_*^2 H_+(\omega v/v_*^2)$ with H_+ some function of the dimensionless argument. In the average-pressure spectrum $Q_0(\omega)$ on a large area ($\omega R_0/U_\infty \gg 1$) in the high-frequency range, the high-wavenumber contribution similarly conforms to the scaling law $Q_{0+}(\omega) = (\pi R_0/v_*)^{-3} \rho^2 v v_*^2 L_+(\omega v/v_*^2)$. The low-wavenumber contribution, if $P(\bar{K}, \omega)$ is wavenumber-white for $K \lesssim 2\pi R_0^{-1}$, conforms rather to the conventional large-area scaling law $Q_{0-}(\omega) = 2(\omega R_0/U_\infty)^{-2} \rho^2 v_*^3 U_\infty^3 G_-(\omega v_*/U_\infty)$, where δ_* is the TBL displacement thickness. The rate of decrease of flow noise with distance aft may be much less than would be inferred from the conventional scaling law.

Unclassified
Security Classification

DOCUMENT CONTROL DATA - R & D		
<i>(Security classification of title, body of abstract and indexing annotation must be entered when the overall report is classified)</i>		
1. ORIGINATING ACTIVITY (Corporate author) TRG, A Division of Control Data Corp. 535 Broad Hollow Road Melville, N.Y.		2a. REPORT SECURITY CLASSIFICATION Unclassified
		2b. GROUP ---
3. REPORT TITLE Dome Effectiveness and the Scaling and Area Dependence of Boundary Layer Pressure Spectra Viewed with Regard to Characteristic Wavenumber Ranges		
4. DESCRIPTIVE NOTES (Type of report and inclusive dates) Technical Report		
5. AUTHOR (First name, middle initial, last name) David M. Chase		
6. REPORT DATE December 1965	7a. TOTAL NO. OF PAGES	7b. NO. OF REFS 7
8a. CONTRACT OR GRANT NO. Nonr 4385(00)	9a. ORIGINATOR'S REPORT NUMBER(S) TRG-011-TN-65-8	
8b. PROJECT NO.	9b. OTHER REPORT NO(S) (Any other numbers that may be assigned to this report) -----	
8c.		
8d.		
10. DISTRIBUTION STATEMENT Distribution of this document is unlimited		
11. SUPPLEMENTARY NOTES ---	12. SPONSORING MILITARY ACTIVITY Department of the Navy Office of Naval Research Washington, D.C. 20360	
13. ABSTRACT Regarding the spectrum of turbulent boundary-layer (TBL) pressure averaged over a flush or shielded area, two distinct wavenumber domains are distinguished: (1) the domain of convection $K > \omega/U_\infty$ [U_∞ = asymptotic flow velocity, $\bar{K} = (K_1, K_3)$] such that boundary-layer eddies of frozen shape convected downstream at speed $u \leq U_\infty$ can generate pressure fluctuations of the given frequency; in this domain the wavenumber-frequency spectrum of TBL pressure $P(\bar{K}, \omega)$ has a broad peak; (2) the domain of relatively low wavenumbers where the response function for pressure on the area in question has its largest magnitude. For a circular flush area of radius R_0 , the contribution to the average-pressure spectrum $Q_0(\omega)$ from the high-wavenumber domain, for $\omega R_0/U_\infty \gg 1$, varies as R_0^{-3} . If $P(\bar{K}, \omega)$ averaged over the angle of \bar{K} is substantially constant (wavenumber-white) for most $K \leq 2\pi R_0^{-1}$, the contribution to $Q_0(\omega)$ from the low-wavenumber domain varies rather as R_0^{-2} . A further low-wavenumber		

DD FORM 1473
NOV 65

Unclassified
Security Classification

Unclassified

Security Classification

10 KEY WORDS	LINK A		LINK B		LINK C	
	ROLE	WT	ROLE	WT	ROLE	WT
Turbulent boundary-layer pressure spectra Domes for flow-noise reduction Scaling of turbulent boundary-layer pressure Area dependence of turbulent boundary-layer pressure						

Unclassified

Security Classification